J.Natn.Sci.Foundation Sri Lanka 2022 50 (2): 453 - 466
DOI: http://dx.doi.org/10.4038/jnsfsr.v50i2.10543

RESEARCH ARTICLE

Earthquake engineering

Seismic performance of stiffened steel box column with different corner stiffener arrangements: a numerical approach

T Thevega*, JASC Jayasinghe and KAS Susantha
Department of Civil Engineering, Faculty of Engineering, University of Peradeniya, Peradeniya, Sri Lanka.

Submitted: 02 June 2021; Revised: 20 January 2022; Accepted: 28 January 2022

Abstract: The purpose of this study is to investigate a stiffening method with numerical analysis to improve the performance of hollow steel box columns, which are commonly and widely used in highway bridges. The major issue with the hollow steel column is local and global buckling at the base under different loadings. There are several methods to prevent local buckling and also to enhance the strength and ductility of the hollow column. Here, the performance of the steel column is improved by adding longitudinal (vertical and corner) and transverse stiffeners inside the column. In this research, the stiffened steel columns are numerically analysed by finite element method incorporating material and geometric non-linearities under constant axial and lateral cyclic loadings. From three different hardening models, the combined hardening material model is used for the steel material for the numerical analysis based on performance. The analytical results clearly show that the strength is improved by stiffening the column in the middle of the plates using vertical stiffeners, and the ductility is improved by stiffening the column at the corners using corner plates. The corner stiffeners avoid faster degradation of strength and also increase the lateral load-carrying capacity at maximum displacement level. It is clear from the numerical results that the overall performance of the hollow steel column is improved with vertical and corner stiffeners.

Keywords: Cyclic analysis, ductility, non-linear finite element analysis, steel column, stiffener arrangements, strength.

INTRODUCTION

Steel columns are commonly used in elevated highway systems because of their high strength and torsional rigidity. Also, the contribution of the steel column becomes important in the construction, as they are cost-effective, sustainable, durable, ductile, and safe. The steel columns are susceptible to damage when subjected to severe lateral deformations that occur due to earthquake loadings. This damage is mainly due to the local buckling of plates and global buckling of the column. In past decades, investigations on the strength and ductility of steel columns under cyclic and dynamic loading have been widely carried out analytically and experimentally by many researchers (Kumar & Usami, 1996; Usami & Ge, 1998; Zheng *et al.*, 2000; Mamaghani, 2004; Aoki & Susantha, 2005).

There are several retrofitting methods introduced by researchers to enhance the strength and ductility capacity of steel columns based on past analytical and experimental studies. One of the commonly used methods is the concrete infilling of steel tubes. In the case of steel bridge piers usually, concrete infilling is done partially, and the height of the concrete-filled in the steel piers can be adjusted to prevent the local buckling (Goto *et al.*, 1998; 2009; Tao *et al.*, 2008; 2015). Linearly tapered thin-walled steel columns can also be used to improve the performance by eliminating severe local buckling near the base of the column (Al-Kaseasbah & Mamaghani, 2019a; 2019b). The steel plates are constructed by different types of welding methods to investigate the sensitivity of ultimate strength and the failure mechanism (Khedmati *et al.*, 2007). To improve the ductility capacity, Low Yield Strength (LYS) steel has been investigated with steel bridge piers (Aoki &

* Corresponding author (thevegat@eng.pdn.ac.lk; https://orcid.org/0000-0001-7939-2876)

Susantha, 2015; He *et al.*, 2015; Li *et al.*, 2020a; 2020b). The effects of different types of stiffener arrangements are studied to prevent local buckling prior to overall buckling and to increase the overall buckling strength (Nishikawa *et al.*, 1998; Zhu *et al.*, 2006; Aizhu *et al.*, 2016; Qian & Astaneh-Asl, 2016).

In the first stage of recent work by Rajavijayan *et al.* (2019), a finite element model has been developed in ABAQUS for a previously tested steel box column (Susantha *et al.*, 2007). The analysis was carried out by simulating the same loading patterns of the experimental data from past literature (Tao *et al.*, 2008) with three different material models, namely, isotropic, kinematic, and combined hardening models. Comparisons were made between the test and predicted results. Then the analyses were repeated for different loading conditions using the combined hardening model, which was found to be the best material model (Rajavijayan *et al.*, 2019). As the second stage of improving the hollow steel columns, different cross-sectional configurations were proposed with constant cross-sectional area by changing the stiffener arrangement inside the column to select the optimum stiffener arrangement. The box column with vertical stiffeners and corner stiffeners are analysed separately. And also, the effects of different lateral cyclic loading patterns were studied with different cross-sections. It was found that the strength of the hollow steel box column could be improved by using the vertical stiffener arrangement, but the ductility was not significantly improved (Thevega *et al.*, 2021). Then corner stiffeners were found to enhance the ductility of the column.

In the present study, steel columns with vertical and corner stiffeners are proposed and numerically analysed to examine their effectiveness in strength and ductility improvement. Here, two cases with corner stiffeners only and a combination of corner stiffeners and vertical stiffeners are considered. The analyses are conducted under constant axial and lateral cyclic loadings.

MATERIALS AND METHODS

The methodology consists of a series of numerical analyses carried out using a finite element model in ABAQUS software, considering the effects of both material and geometric non-linearities. The reliability of prediction of this type of investigation highly depends on the details of the finite element model, such as material models, element types, mesh, boundary conditions, and solution technique. The finite element model was analysed with different hardening material models. A suitable material model was selected to do further analyses after comparing numerical results with the experimental result. After that, three sets of columns with different cross-sectional configurations, designed by changing the number of vertical stiffeners and length of corner stiffeners, were analysed under lateral cyclic loading. Finally, the strength and ductility were compared using the envelope curves of these hysteretic curves.

Cross-sectional details

The vertical stiffeners are important to improve the performance of the column (Rajavijayan *et al.*, 2019). In addition, when the number of stiffeners of the same size is increased, the performance of the column improves. Figure 1 clearly shows the performance of the column (450 mm × 450 mm) with different numbers of stiffeners (n), which are the same size (length of the stiffener = 53 mm, the thickness of the plate and the stiffener = 5.8 mm). According to that, the cross-sections with two and four vertical stiffeners, with the same size of stiffeners, were selected for further analyses with different lengths of corner stiffeners.

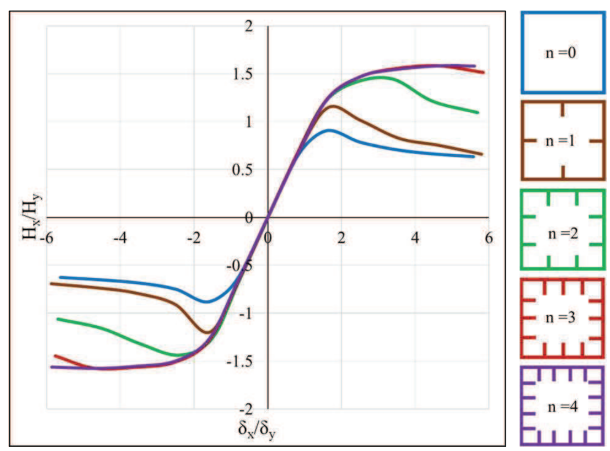

Figure 1: The variation of lateral force with lateral displacement (envelope curves)

Sixteen different cross-sectional configurations are proposed to investigate the effects of corner stiffeners and the combination of corner stiffeners with vertical stiffeners. All cross-sections are maintained as 450 mm × 450 mm in outer size. The height of the column is 2420 mm. In addition to the longitudinal stiffeners, three horizontal stiffeners (diaphragms) are provided at intervals of about 450 mm from the base of the column.

All the steel plates have welded connections (main plates, longitudinal stiffeners and transverse stiffeners). In this research, there are three different sets considered. In column Set-1, five cross-sections (C1-C5) are selected with only corner stiffeners by changing the length of the corner stiffener (cross-sectional configuration for the hollow box column is kept, as shown in Figure 2). The cross-sectional details are given in Table 1. The other two sets are defined with vertical and corner stiffeners.

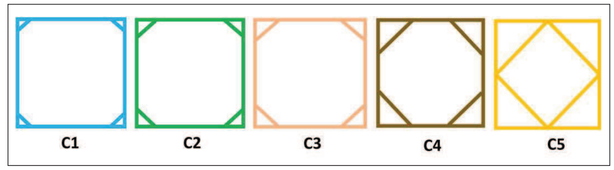

Figure 2: Different corner stiffeners arrangement in Set-1

Table 1: Cross-sectional details of the columns in Set-1

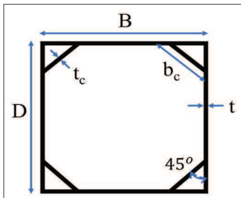

Cross-section	B,D (mm)	t (mm)	b_c (mm)	t_c (mm)
C1	450	5.8	59.5	5.8
C2	450	5.8	89.3	5.8
C3	450	5.8	119.0	5.8
C4	450	5.8	201.2	5.8
C5	450	5.8	310.0	5.8

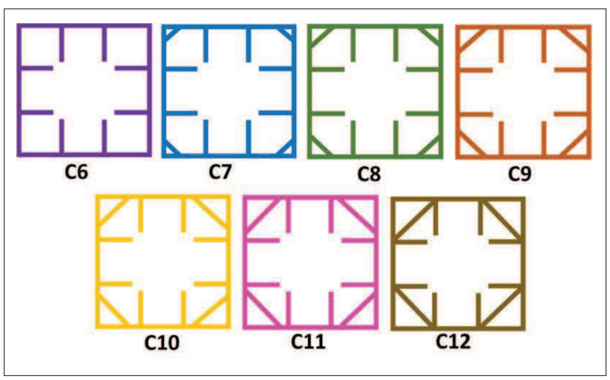

Figure 3: Different corner stiffener arrangements with vertical stiffeners in Set-2

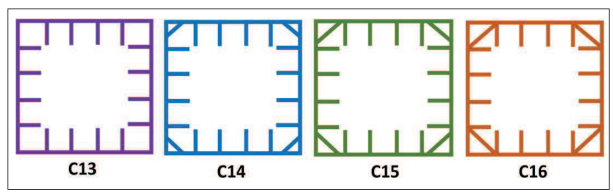

Figure 4: Different corner stiffener arrangements with vertical stiffeners in Set-3

Set-2 consists of columns (C6-C12) with two vertical stiffeners with corner stiffeners, and Set 3 includes the columns (C13-C16) with four vertical stiffeners with corner stiffeners. The corner stiffeners are inserted in different lengths to study the effect of the corner stiffeners on the vertical stiffeners. The inclination of corner stiffeners with the outer plate is kept constant at 45 degrees for all the cases, as shown in Figures 3 and 4. Tables 2 and 3 show the cross-sectional details of columns Set-2 and Set-3.

Table 2: Cross-sectional details of the columns in Set-2

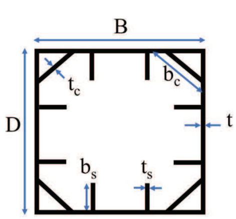

Cross-section	B,D (mm)	t (mm)	b_s (mm)	t_s (mm)	b_c (mm)	t_c (mm)
C6	450	5.8	53	5.8	-	-
C7	450	5.8	53	5.8	59.5	5.8
C8	450	5.8	53	5.8	89.3	5.8
C9	450	5.8	53	5.8	119.0	5.8
C10	450	5.8	53	5.8	144.0	5.8
C11	450	5.8	53	5.8	169.7	5.8
C12	450	5.8	53	5.8	201.2	5.8

Material model

For the proposed non-linear analysis procedure, both geometric and material non-linearity need to be incorporated as the columns are expected to deform beyond several times their yield displacement. Yield surface, flow rule, and stress-strain envelope of uni-directional loading curves are important in numerical simulation of material behaviour. Von Mises, Tresca, and Mohr-Coulomb are some yield criteria to define the yield surface where material undergoes yielding. The Von Mises yield criterion is commonly used in steel material models. The steel material can be differentiated with three different hardening rules (4) in the inelastic range, such as Isotropic Hardening (IH), Kinematic Hardening (KH) and Combined Hardening (CH). The IH rule states that the yield surface expands proportionally in all directions when stress exceeds its yield stress. The KH involves a translation of the yield surface without expansion of the surface. It is known as the Bauschinger effect. The CH rule states that the yield surface expands and translates in the direction of the stress rising.

Material properties

Three hardening material models were used with bilinear stress-strain material (see Figure 5). The bilinear stress-strain model was assumed from the trilinear material model, as shown in Figure 5. The steel material of grade SM490 (JIS - Japanese Industrial Standard) (Susantha *et al.*, 2001), with material properties of yield stress (σ_y) = 412 MPa, Young modulus (E_s) = 206,000 MPa, Poisson ratio (v) = 0.276, $\varepsilon_{st}/\varepsilon_y$ (Elastic strain/Yield strain) = 7, and E_{st}/E_s (Secant modulus/Tangent modulus) = 1/30 were used for the main plates, stiffeners and diaphragms.

Finite element model

The stiffened steel columns were modelled using the 4 node shell elements (S4R) in the ABAQUS program. The mesh sensitivity on the result was tested first, and the optimum element mesh was selected to maintain the accuracy of results and good computational efficiency. This is very important because the analyses involve severe

Table 3: Cross-sectional details of the columns in Set-3

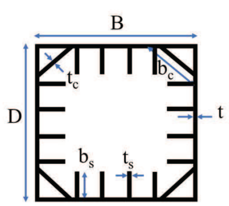

Cross-section	B,D (mm)	t (mm)	b_s (mm)	t_s (mm)	b_c (mm)	t_c (mm)
C13	450	5.8	53	5.8	-	-
C14	450	5.8	53	5.8	59.5	5.8
C15	450	5.8	53	5.8	89.3	5.8
C16	450	5.8	53	5.8	119.0	5.8

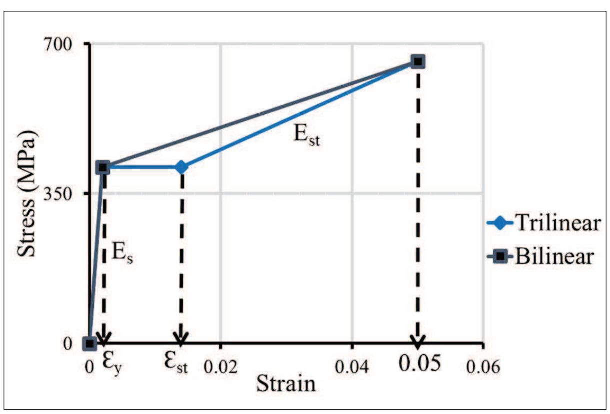

Figure 5: Stress-Strain relationship of steel

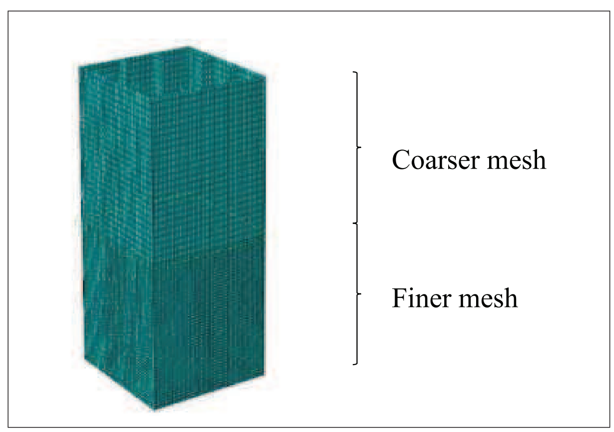

Figure 6: Finite element mesh

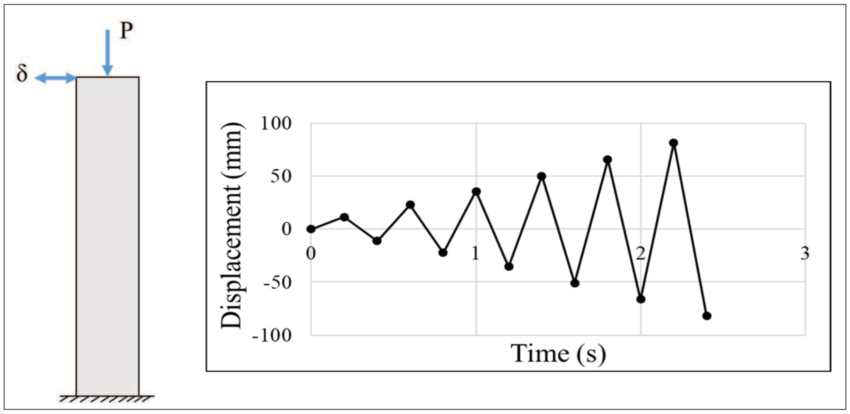

Figure 7: The loading arrangement on the column

non-linearity and are to be conducted for several cycles where each cycle needs a large number of increments. As a result, a finer mesh at the bottom where high stresses and buckling are expected and a coarser mesh at the top of the column were selected, as shown in Figure 6. All nodes at the bottom of the column are fixed.

Loading arrangement

For the numerical analysis, the loading arrangement used is the same as the experimental arrangement of the column in Susantha *et al.* (2007) (see Figure 7). First, the axial load (P = 0.2 P_y, $P_y = A_s\sigma_y$, where P_y is the yield axial load, A_s is the cross-sectional area and σ_y is the yield stress of steel) is applied at the top of the column, and next, lateral cyclic displacements are incrementally applied at the top for all the columns. The same loading pattern was employed for all the columns that have different cross-sectional configurations.

RESULTS AND DISCUSSION

Numerical simulation of stiffened steel box columns

The lateral load-lateral displacement hysteretic curves were normalized by corresponding yield load H_y and yield displacement δ_y (Susantha *et al*., 2007), given in equations 1 and 2.

$$H_y = \frac{M_y}{h}\left(1 - \frac{P}{P_y}\right) \quad ...(1)$$

$$\delta_y = \frac{H_y h^3}{3EI} \quad ...(2)$$

Where,

H_y = Lateral yield load, δ_y = Lateral yield displacement, M_y = Bending moment at yield load, P = Axial load, P_y = Yield axial load, h = Height of column, E = Young's modulus, and I = Second moment of inertia

The value of M_y is computed from equation 3.

$$M_y = \frac{\sigma_y I}{h} \quad ...(3)$$

Validation and selection of the material model

Analyses were conducted using all three hardening models (IH, KH, and CH). The experimental result (Susantha *et al.*, 2007) and predicted results using IH, KH, and CH models were compared. It was found that among the three models, the CH model gave a relatively better comparison with experimental results, and a large difference in lateral load capacity was observed with the IH model (see Figure 8). Also, the combined hardening material model was performed as a combination of isotropic hardening and kinematic hardening material. Therefore, the CH model was identified as the most suitable material model to be used in the rest of the finite element analyses.

The performance of columns with only corner stiffeners

The results of the lateral load-lateral displacement curves of column Set-1 having different corner stiffener arrangements are shown in Figures 9 and 10. As shown in Figure 9, it is proved by using lateral load - lateral displacement curves without normalizing that the initial

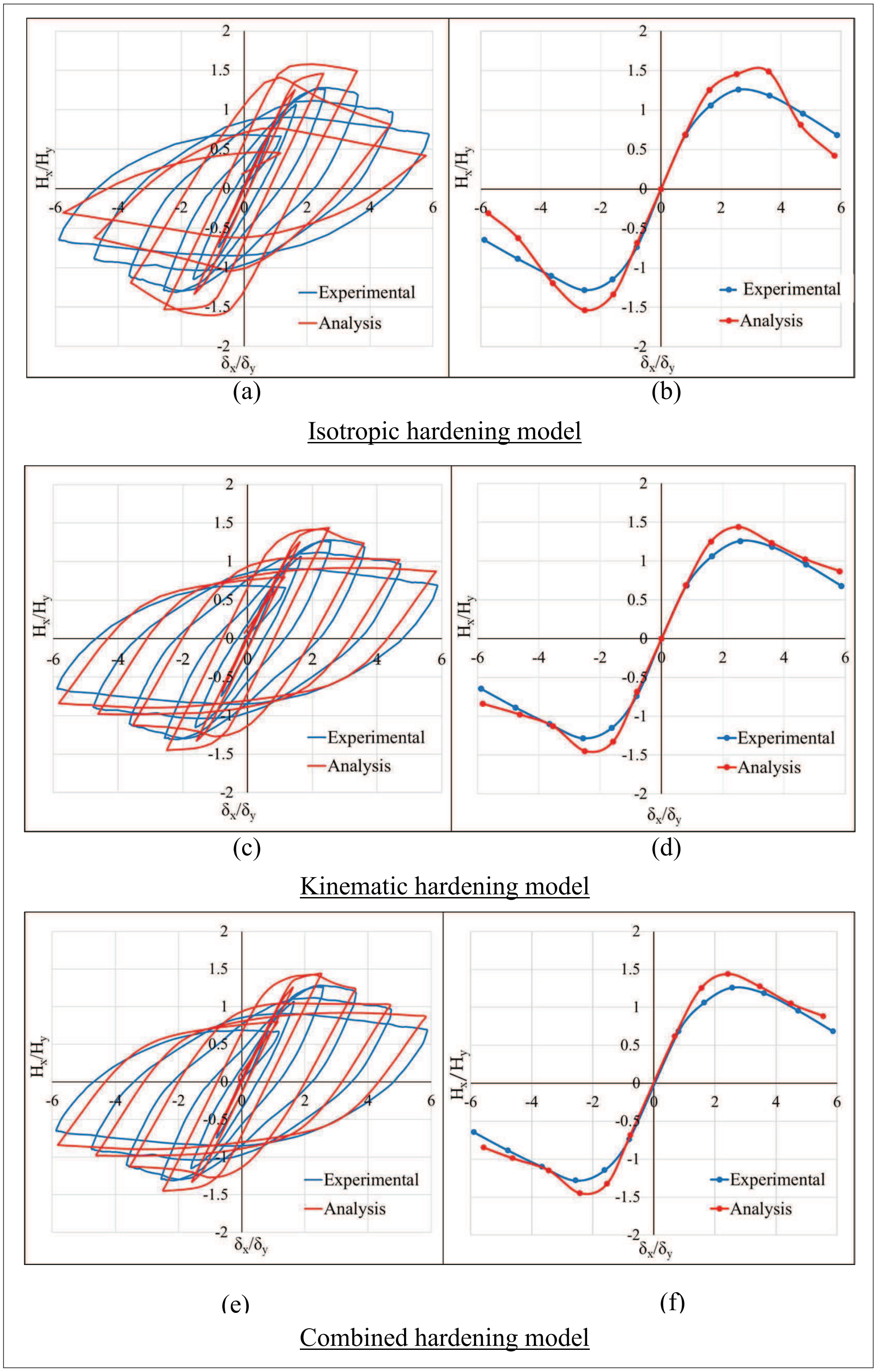

Figure 8: Normalized lateral load-lateral displacement curves (experimental versus analyses): (a) IH hysteresis, (b) IH envelope, (c) KH hysteresis, (d) KH envelope, (e) CH hysteresis and (f) CH envelope

stiffness of the columns increases with the length of the corner stiffeners. This fact should also be considered when deciding on the optimum cross-sectional shape. When the length of the corner stiffeners was increased, strength and ductility increased. However, when the length of the stiffener reaches its maximum while maintaining the same angle with outer plates, the maximum lateral load capacity is reduced.

The strength of the column is defined by index (H_m /H_y), where H_m is the maximum lateral load (Ucak & Tsopelas, 2006). The cross-section type C4 gives the maximum strength. But the cross-section C3 performs better than C4 at the maximum lateral displacement as corner stiffeners start to buckle (see Figure 10). And also, the performance of the cross-section C4 is less than C2 between displacement levels of 4δ_y and 5δ_y.

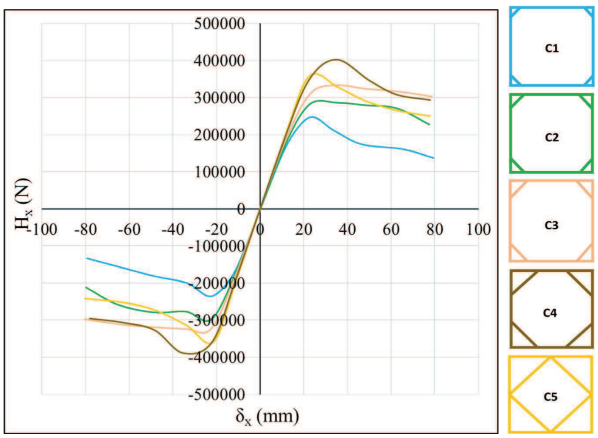

Figure 9: Lateral load versus lateral displacement curves for different corner stiffener arrangements

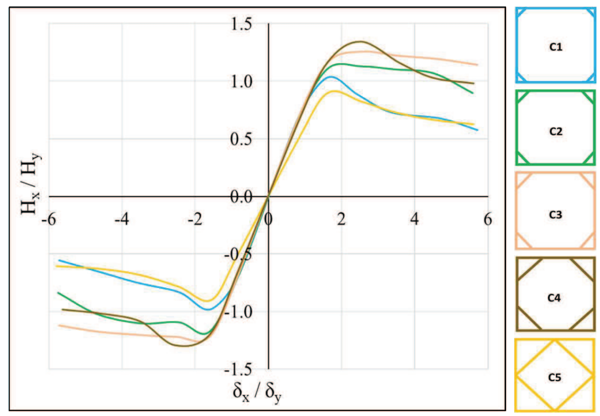

Figure 10: Normalized lateral load versus lateral displacement curves (Envelope curves) for Set-1

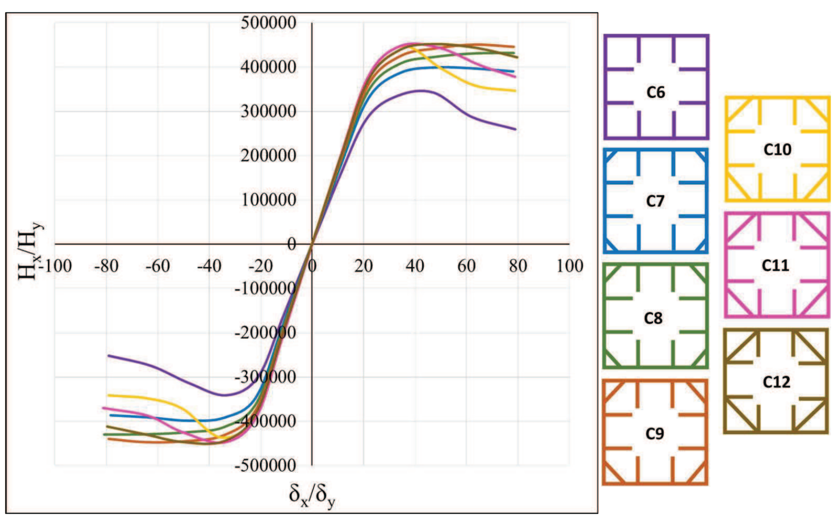

Figure 11: Lateral load versus lateral displacement curves for different corner stiffener arrangements with two vertical stiffeners

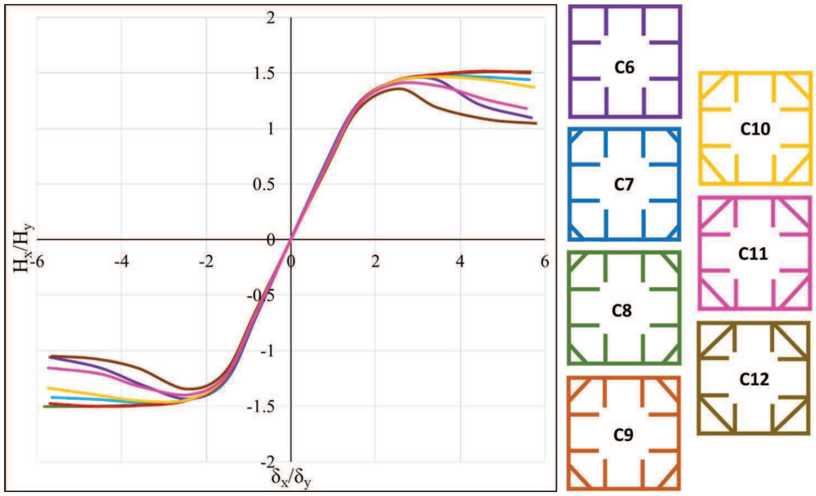

Figure 12: Normalized lateral load versus lateral displacement curves (Envelope curves) for Set-2

The performance of columns with two vertical stiffeners and corner stiffeners

Next, the effects of different corner stiffener arrangements with two vertical stiffeners were analysed. Figure 11 illustrates that the performance of the column is enhanced by increasing the second moment of area of the column in the elastic range. But the strength and ductility do not depend on the second moment of area in the plastic range.

After normalizing, the variation of lateral load with lateral displacement is shown in Figure 12. It clearly shows that the ductile behaviour is improved with corner stiffeners. However, it depends on the length of the corner stiffeners. The maximum lateral load capacity of cross-section C12 is less than that of cross-section C6. Even though the length of the corner stiffener in cross-section C9 is less than that in cross-sections C10, C11, and C12, the performance of C9 is high. The strength and ductility are improved with cross-section C9 when compared with other cross-sections.

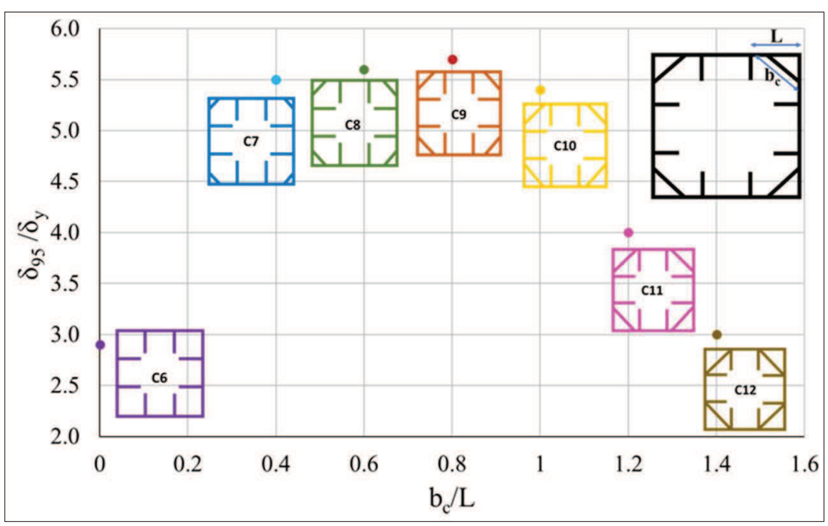

Figure 13: The variation of ductility index with different cross-sectional configurations of Set-2

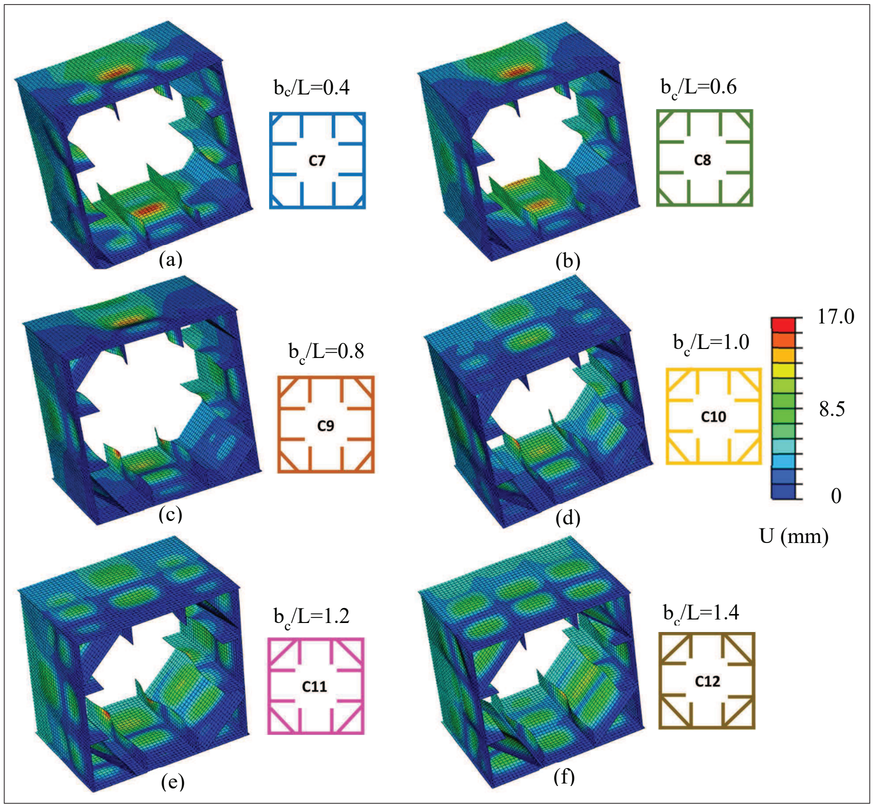

Figure 14: Deformed shapes for different cross-sectional arrangement of Set-2

After a particular length, the corner stiffener does not enhance the ductility of the column. The performance is drastically reduced, similar to the column without corner stiffeners. The strength of the cross-section C12 (with a maximum length of corner stiffener) is less than C6 (without corner stiffener). Therefore, it is important to select a length for a corner stiffener to be used effectively. There are two definitions for ductility (Gao & Ge, 2000; Aoki & Susantha, 2005) which can be defined as the ratio of lateral displacement at the maximum load to yield displacement (δ_m/δ_y) and the ratio of lateral displacement at 95% of the maximum load to yield displacement (δ_{95}/δ_y). Figure 13 shows the variation of the ductility index (δ_{95}/δ_y) with the ratio of the length of corner stiffener and space between vertical stiffeners (b_c /L) in Set-2. It is apparent that the ductility is drastically increased with different lengths of corner stiffeners, and also it is reduced by increasing the length of the corner plates. When the b_c /L ratio is equal to 0.8, the ductility is high as 5.7.

The buckling shapes are obtained at the end of the lateral displacement level for different cross-sectional configurations, as shown in Figure 14. It clearly shows that when b_c/L is less than 0.8, the outer plates start to buckle with vertical stiffeners prior to the corner plates. At b_c/L = 0.8, the corner stiffeners start to buckle. After that, outer plates, vertical stiffeners, and corner stiffeners perform together under cyclic loading.

The performance of columns with four vertical stiffeners and corner stiffeners

Finally, the effects of different corner stiffener arrangements with four vertical stiffeners were investigated. The lateral load - lateral displacement curves without normalizing are shown in Figure 15. It clearly shows that the maximum strength increases with the cross-sectional area of the columns.

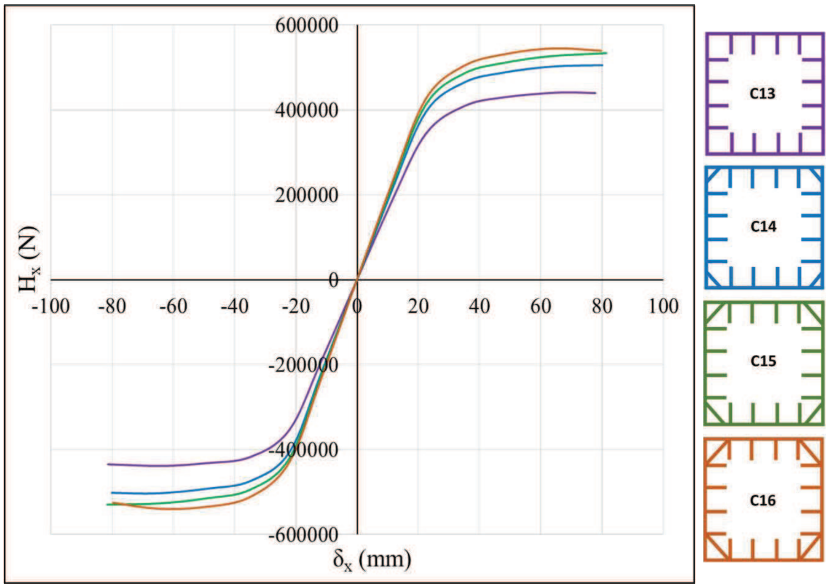

Figure 15: Lateral load versus lateral displacement curves for different corner stiffener arrangements with four vertical stiffeners

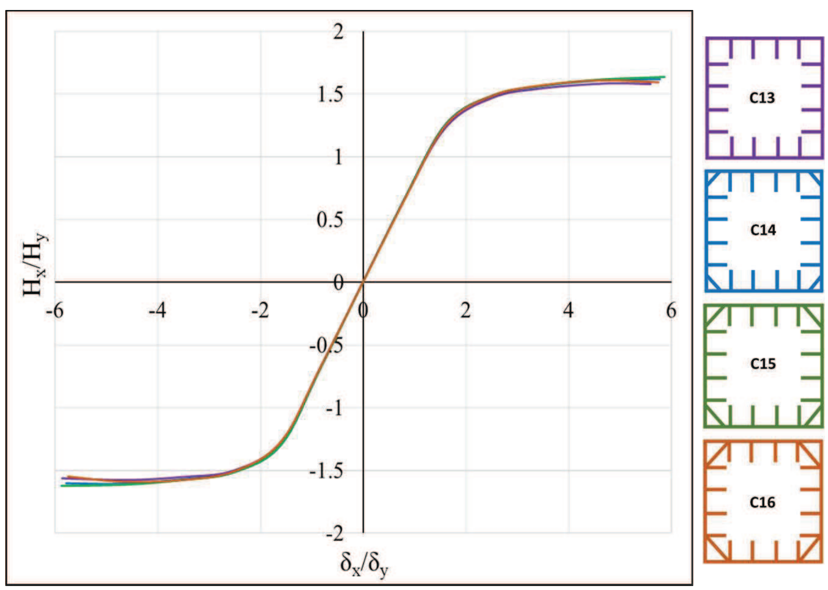

Figure 16: Normalized lateral load versus lateral displacement curves (Envelope curves) for Set-3

After normalizing by corresponding yield load H_y and yield displacement δ_y, the variation of lateral load with lateral displacement is shown in Figure 16. It clearly shows that the lateral load capacity and ductility are nearly the same for all cross-sections C13, C14, C15, and C16. Before normalizing, the lateral load capacity increases with the second moment of area (see Figure 15). However, it is clear from Figure 16 that the performance of columns with four vertical stiffeners and corner stiffeners is approximately the same for all, even though the length of the corner stiffeners is different.

The variation of the ductility index (δ_{95}/δ_y) with (b_c/L) of Set-3 is shown in Figure 17. The ductility, which is slightly increased with the length of the corner stiffener, is high when b_c/L is 1.1. When the length of the corner stiffener increases from 59.5 to 89.3 mm with the same size of vertical stiffeners, the ductility index increases from 5.8 to 5.9 and the length of the corner stiffener increases from 89.3 to 119.0 mm with the same size of vertical stiffeners, the ductility index decreases from 5.9 to 5.7.

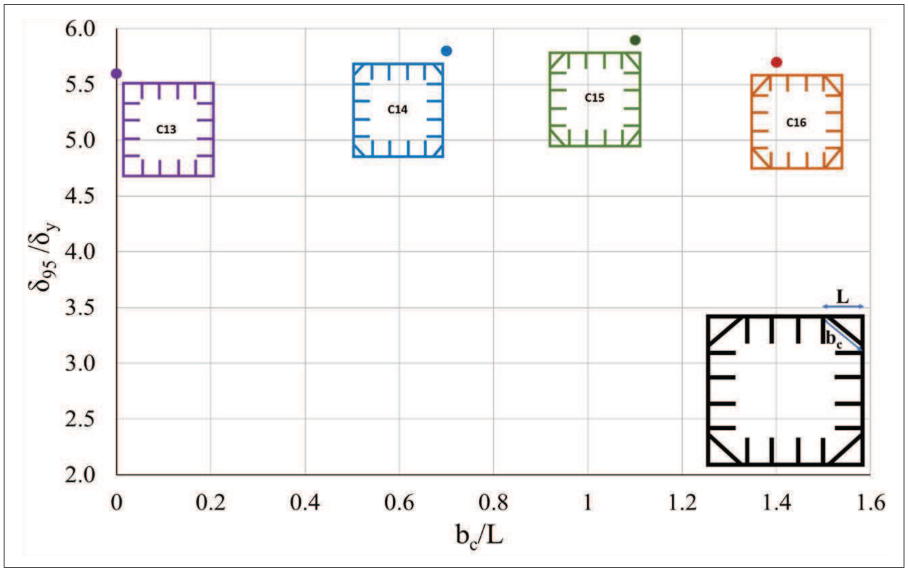

Figure 17: The variation of ductility index with different cross-sectional configurations of Set-3

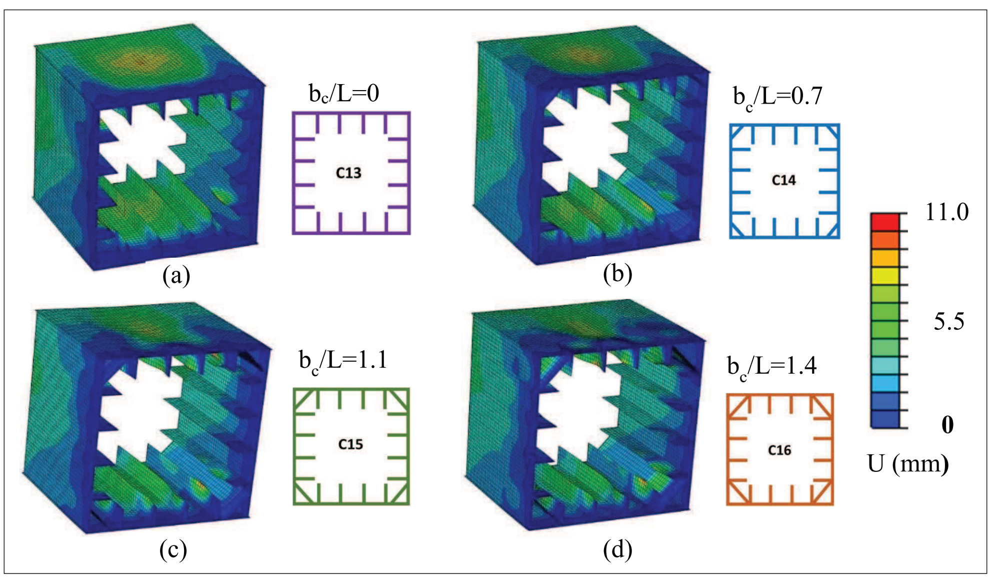

Figure 18: Deformed shapes for the different cross-sectional arrangement of Set-3

The deformed shape is obtained at the end of the lateral displacement level for different cross-sectional configurations, as shown in Figure 18. The buckling modes are comparatively the same for all cross-sections in column Set-3. Even though the length of corner stiffeners changes with cross-section, all cross-sections deform similarly. When the lateral load is applied, outer plates, vertical stiffeners, and corner stiffeners bear the load and delay the buckling.

Table 4 shows the comparison of strength and ductility of all cross-sections in columns Set-1, Set 2 and Set-3. The performance of the column depends on the number of stiffeners and the size of the stiffeners. And also, the b_c/L ratio plays a major role in the columns with corner stiffeners. The cross-sections C9 and C15 show better performance in Set-2 and Set-3, respectively. However, the performance of the cross-section C15 is higher than other cross-sections.

Table 4: The comparison of strength and ductility index of column Set-2 and Set-3

Cross-sections	b_c/L	H_m/H_y	δ_{95}/δ_y
C1	0.1	1.03	2.0
C2	0.2	1.15	3.4
C3	0.3	1.25	4.0
C4	0.5	1.34	2.9
C5	0.7	0.92	2.2
C6	0	1.45	2.9
C7	0.4	1.48	5.5
C8	0.6	1.50	5.6
C9	0.8	1.52	5.7
C10	1.0	1.47	5.4
C11	1.2	1.42	4.0
C12	1.4	1.36	3.0
C13	0	1.58	5.6
C14	0.7	1.62	5.8
C15	1.1	1.64	5.9
C16	1.4	1.60	5.7

CONCLUSIONS

In this study, numerical analyses have been conducted to examine the performance of steel hollow box columns by stiffening the outer plates with vertical and corner stiffeners arranged longitudinally. The analyses were conducted using the non-linear large deformation finite element method with the help of ABAQUS. Primarily, three sets of columns are considered as (1) Set-1: only corner stiffeners; (2) Set-2: corner stiffeners and two vertical stiffeners and (3) Set-3: corner stiffeners and four vertical stiffeners. The following are drawn as the key conclusions of this study.

The cross-sections having only corner stiffeners contribute significantly to increasing the ductility compared with those having only vertical stiffeners. However, the strength increase with corner stiffeners alone is lower than those with vertical stiffeners. Therefore, it is important to have vertical stiffeners to increase the strength (maximum lateral load).

In column Set-1, the size (length) and the arrangement of corner stiffeners play a major role in the ductility performance of columns. Increasing the length abruptly will not yield favourable results, as seen in the case of cross-section C5. There is an optimum length for the best performance.

With only corner stiffeners, after buckling, the strength gradually decreases, but with both types of stiffeners, there is no reduction in strength, and also ductility is greatly improved. Therefore, providing a combination of stiffeners (vertical and corner stiffeners) will give a more favourable performance.

The results of columns in Set-2 show the importance of the length of the corner stiffener. The strength and ductility depend on the length of the corner stiffener. When b_c/L increases from 0 to 0.8, the ductility increases by 97% and the strength increases by 5%. However, when b_c/L increases further from 0.8 to 1.4, there is a drastic drop in the performance. Even though the cross-section C12 has a larger length of corner stiffener, it was not useful for improving strength with corner plates. There is a huge difference in the lateral load capacity of C12, which is 7% less than C6 (without corner stiffener).

1. In column Set-3, the ductile behaviour of cross-section types C14, C15, and C16 is slightly better than that of cross-section C13 (without corner stiffeners).

And also, the maximum lateral load capacity, which is achieved, is nearly the same for all cross-sections. However, the cross-section C15 (b_c/L = 1.1) has high strength and ductility, which are increased by 4% and 6 % respectively compared to C13 (b_c/L = 0).

2. While comparing the performance of all cross-sections, the cross-section C15 with four vertical stiffeners and corner stiffeners (b_c/L =1.1) can be selected for enhanced strength and ductility. When the column with cross-section C15 is compared with the column without stiffener (only having outer plates), there is a huge improvement in strength and ductility, by 41% and 181%, respectively.
3. When the length of the corner stiffener increases, the corner stiffeners perform together with the vertical stiffeners and outer plates. Therefore, the performance of columns with vertical and corner stiffeners depends on the b_c/L ratio. When b_c/L is equal to 0.8, the column shows high performance with two vertical stiffeners, and when b_c/L is equal to 1.1, the capacity is improved with four vertical stiffeners.

The strength and ductility of the column are enhanced with vertical and corner stiffeners. The length of the corner stiffener plays a major role with a given number of vertical stiffeners, and also different values perform optimally with different numbers of vertical stiffeners. From the numerical analyses, the number of stiffeners and the size of stiffeners can be selected to construct the column effectively.

Acknowledgement

The authors would like to express their acknowledgement for licensed applications of the ABAQUS package facilitated by the Finite Element Analysis and Simulation Centre, Rubber Research Institute of Sri Lanka, Ratmalana.

REFERENCES

Aizhu, Z., Hongping, Z., Xiaowu, Z. & Yong L. (2016). Experimental study and analysis of inner stiffened cold-formed SHS steel stub columns. *Thin-walled Structures* **107**: 28–38.
DOI: https://doi.org/10.1016/j.tws.2016.04.026

Al-Kaseasbah Q. & Mamaghani P.H.I. (2019a). Design and cyclic elastoplastic analysis of graded thin-walled steel tubular columns with enhanced strength and ductility. *International Journal of Modern Engineering* **19**.

Al-Kaseasbeh Q. & Mamaghani P.H.I. (2019b). Buckling strength and ductility evaluation of thin-walled steel stiffened square box columns with uniform and graded thickness under cyclic loading. *Engineering Structures* **186**: 498–507.
DOI: https://doi.org/10.1016/j.engstruct.2019.02.026

Aoki T. & Susantha K.A.S. (2005). Seismic performance of rectangular-shaped steel piers under cyclic loading. *Journal of Structural Engineering* **131**(02): 240–249.
DOI: https://doi.org/10.1061/(ASCE)0733-9445(2005)131:2(240)

Aoki T. & Susantha S. (2015). Application of low yield strength steel in steel bridge piers. *13th Conference on Earthquake Engineering*, Paper No. 339.

Gao S. & Ge H. (2000). Eccentrically loaded steel columns under cyclic in-plane loading. *Journal of Structural Engineering* **126**(08).
DOI: https://doi.org/10.1061/(ASCE)0733-9445(2000)126:8(964)

Goto Y., Kumar P.G. & Kawanishi N. (2009). FEM analysis for hysteretic behavior of CFT bridge piers considering interaction between steel tube and infilled concrete. *Japan Society of Civil Engineers* **65**(02): 487–504.
DOI: https://doi.org/10.2208/jsceja.65.487

Goto Y., Wang Q. & Obata M. (1998). FEM analysis for hysteretic behavior of thin-walled columns. *Journal of Structural Engineering* **124**(11): 1290–1301.
DOI: https://doi.org/10.1061/(ASCE)0733-9445(1998)124:11(1290)

He H., Chen K. & Li R. (2015). Seismic performances of replaceable steel connection with low yield point metal. *Advances in Materials Science and Engineering* **2015**: Article ID 134189.
DOI: https://doi.org/10.1155/2015/134189

Khedmati M.R., Ghavami K. & Rastani M. (2007). A comparative study on three different construction methods of stiffened plates strength behavior and ductility characteristics. *Revista Escola de Minas Ouro Preto* **60**(02): 365–379.
DOI: https://doi.org/10.1590/S0370-44672007000200019

Kumar S. & Usami T. (1996). Damage evaluation in steel box columns by cyclic loadings. *Journal of Structural Engineering* **122**(06).
DOI: https://doi.org/10.1061/(ASCE)0733-9445(1996)122:6(626)

Li H., Lv K. & Cui R. (2020a). Seismic behavior of eccentrically compressed steel-box bridge-pier columns with embedded energy-dissipating shell plates. *Bulletin Earthquake Engineering* **18**(7): 3401–3432.
DOI: https://doi.org/10.1007/s10518-020-00830-2

Li H., Luo W. & Luo J. (2020b). Seismic performance of steel box bridge piers with earthquake-resilient function. *Advances in Civil Engineering* **2020**: Article ID 8877785.
DOI: https://doi.org/10.1155/2020/8877785

Mamaghani P.H.I. (2004). Seismic design and retrofit of thin-walled steel tubular columns. *13th World Conference on Earthquake Engineering*, Paper No. 271.

Nishikawa K., Yamamoto S., Natori T., Terao K., Yasunami H. & Terada M. (1998). Retrofitting for seismic upgrading of steel bridge piers. *Engineering Structures* **20**: 540–551.

DOI: https://doi.org/10.1016/S0141-0296(97)00025-4

Qian X. & Astaneh-Asl A. (2016). Behavior and seismic design of stiffeners for steel bridge tower legs and piers. *Proceedings of the World Congress on Civil, Structural, and Environmental Engineering (CSEE'16),* Paper No. ICSENM 117.
DOI: https://doi.org/10.11159/icsenm16.117

Rajavijayan K., Thevega T., Jayasinghe J.A.S.C. & Susantha K.A.S. (2019). Performance of steel bridge piers using lateral cyclic load analysis. *10th International Conference on Structural Engineering and Construction Management* **2**: 251–257.

Susantha K.A.S., Ge H. & Usami T. (2001). A capacity prediction procedure for concrete-filled steel columns. *Journal of Earthquake Engineering* **5**(04): 483–520.
DOI: https://doi.org/10.1080/13632460109350403

Susantha S., Aoki T. & Jayasinghe R.T.M. (2007). Finite element analysis of steel columns subjected to bi-directional cyclic loads. *Journal of the Institution of Engineers, Sri Lanka* **40**(04): 35–41.
DOI: https://doi.org/10.4038/engineer.v40i4.7152

Tao Z., Han L.H. & Wang D.Y. (2008). Strength and ductility of stiffened thin-wall hollow steel structural stub columns filled with concrete. *Thin-wall Structures* **46**(10): 1113–1128.
DOI: https://doi.org/10.1016/j.tws.2008.01.007

Tao Z., Han L.H. & Wang D.Y. (2015). Experimental behavior of stiffened concrete-filled thin-walled hollow structural steel (HSS) stub column. *Journal of Constructional Steel Research* **61**: 962–983.
DOI: https://doi.org/10.1016/j.jcsr.2004.12.003

Thevega T., Rajavijayan K., Jayasinghe J.A.S.C. & Susantha K.A.S. (2021). Strength and ductility of stiffened steel box columns of various cross-sectional configurations under lateral cyclic loadings. *Journal of the Institution of Engineers, Sri Lanka* **LIV**(02): 25–32.
DOI: https://doi.org/10.4038/engineer.v54i2.7440

Ucak A. & Tsopelas P. (2006) Cellular and corrugated cross-sectioned thin-walled steel bridge- piers/columns. *Structural Engineering and Mechanics* **24**(03): 355–374.
DOI: https://doi.org/10.12989/sem.2006.24.3.355

Usami T. & Ge B.H. (1998). Cyclic behavior of thin-walled steel structures - numerical analysis. *Thin-walled Structures* **32**: 41–80.
DOI: https://doi.org/10.1016/S0263-8231(98)00027-5

Zheng Y., Usami T. & Ge H. (2000). Ductility of thin-walled steel box stub columns. *Journal of Structural Engineering* **126**(11).
DOI: https://doi.org/10.1061/(ASCE)0733-9445(2000)126:11(1304)

Zhu A., Zhu H., Zhang X. & Lu Y. (2006). Experimental study and analysis of inner-stiffened cold-formed SHS steel stub columns. *Thin-walled Structures* **106**: 28–38.
DOI: https://doi.org/10.1016/j.tws.2016.04.026